



1 **Comment on “Estimating the depth and evolution of intrusions at resurgent**
2 **calderas: Los Humeros (Mexico)” by Urbani et al. (2020)**

3
4
5
6
7
8
9

Gianluca Norini and Gianluca Groppelli

Istituto di Geologia Ambientale e Geoingegneria, Sezione di Milano, Consiglio Nazionale delle Ricerche, Italy

Correspondence: Gianluca Norini (gianluca.norini@cnr.it)

10 **Abstract**

11 A multiple shallow-seated magmatic intrusions model has been proposed by Urbani et al. (2020) for the
12 resurgence of the Los Potreros caldera floor, in the Los Humeros Volcanic Complex. This model predicts (1)
13 the occurrence of localized bulges in the otherwise undeformed caldera floor, and (2) that the faults
14 corresponding to different bulges exhibit different spatial and temporal evolution. Published data and a
15 morphological analysis show that these two conditions are not met at Los Potreros caldera. A geothermal
16 well (H4), located at the youngest supposed bulge (Loma Blanca) for which Urbani et al. (2020) calculated an
17 intrusion depth (425 ± 170 m), doesn't show any thermal and lithological evidence of such a shallow-seated
18 cryptodome. Finally, published stratigraphic data and radiometric dating disprove the proposed common
19 genesis of Holocene resurgence faulting and viscous lavas extruded in the centre of the caldera. Even if recent
20 shallow intrusions may exist in the area, published data indicate that the pressurization of the LHVC
21 magmatic/hydrothermal system driving resurgence faulting occurs at greater depth. Thus, we suggest that
22 the model and calculation proposed by Urbani et al. (2020) are unlikely to have any relevance to the location,
23 age and emplacement depth of magma intrusions driving resurgence at the Los Potreros caldera.

24

25 **1 Introduction**

26 Urbani et al. (2020) (henceforth U2020) made a contribution to the study of caldera resurgence based on
27 field data and geothermal well logs from the Los Humeros Volcanic Complex (LHVC) and scaled analogue
28 models. U2020 constrained the spatial-temporal evolution of post-caldera volcanism at LHVC and estimate
29 the depth of the magmatic intrusions feeding the active geothermal system by integrating fieldwork data,
30 well logs and laboratory results. The main conclusion of U2020 is that the resurgence of the Los Potreros
31 caldera in the LHVC “*is due to multiple deformation sources*”, “*linked to small magmatic intrusions located at*
32 *relatively shallow depths (i.e. < 1 km)*”. U2020 suggested that these intrusions are located below three
33 uplifted areas surrounding the Arroyo Grande, Los Humeros and Loma Blanca faults, respectively.

34 The analysis by U2020 suffers from poor field data and contradictions with thermal remote sensing data
35 (Section 2), geometric and structural inconsistencies between the LHVC post-caldera deformation and the
36 analogue modelling (Section 3), lack of any substantial validation of the results with published well logs
37 (Section 4), and incongruities with the reference stratigraphy and radiometric ages recently published by
38 some of the U2020 authors (Section 5). These problems, which largely undermine the U2020 conclusions,
39 are discussed below.

40



41 **2 Location and relative age of faulting: field data and thermal remote sensing**

42 U2020 analysed the occurrence and relative age of faulting, and proposed a new interpretation of some
43 structures identified by previous works, by studying faults and hydrothermal alteration in the Holocene
44 Cuicuiltic Member unit (Ferriz and Mahood, 1984; Arellano et al., 2003; Dávila–Harris and Carrasco–Núñez,
45 2014; Norini et al., 2015, 2019). The Cuicuiltic Member blankets the Los Potreros caldera floor (Fig. 1), is very
46 well exposed, has been dated at ca. 7 ka and is made of alternated fallout deposits of different composition
47 (Dávila–Harris and Carrasco–Núñez, 2014). The Cuicuiltic Member has been considered an ideal marker layer
48 for documenting Holocene faulting and stratigraphy in the caldera complex, because of the contrasting black
49 and white colours of the fallout deposits composing the unit (e.g. Ferriz and Mahood, 1984; Dávila–Harris
50 and Carrasco–Núñez, 2014; Norini et al., 2015, 2019; GEMex, 2019; U2020) (Figs. 1 and 2). The
51 reinterpretation by U2020 has been based on their field data (22 fault data in 3 outcrops), distinguishing
52 between lineaments (“*morphological linear scarps with no measurable fault offsets and/or alteration at the*
53 *outcrop scale*”) and active and inactive faults (“*associated with measurable fault offsets and with active or*
54 *fossil alteration*”), respectively. The reinterpreted structures are the Las Papas, Las Viboras, Arroyo Grande
55 and Maxtaloya faults (Fig. 1).

56 We discuss the U2020 reinterpretation below, considering published field data (175 fault data in 24 outcrops,
57 Figs. 1 and 2, Tab. 1) and thermal remote sensing data (Fig. 3) (Norini et al., 2015, 2019; GEMex, 2019).

58

59 **2.1 Las Papas and Las Viboras faults**

60 U2020 concluded that the Las Papas and Las Viboras are “*morphological scarps*” and “*lineaments*” not related
61 to faulting. For the Las Papas lineament, U2020 stated that “*unaltered and undeformed deposits of the*
62 *Cuicuiltic Member crop out along the E–W Las Papas lineament*” and that it “*is probably due to differential*
63 *erosion of the softer layers of the pyroclastic deposits*”. Even if the Las Papas and Las Viboras structures were
64 several km long, the statements by U2020 have only been based on one outcrop on the Las Papas trace
65 (U2020 LH–08 outcrop, while the LH–07 outcrop is out of the fault trace; see Fig. 4C).

66 Several outcrops exist along the Las Papas and Las Viboras faults, as well as along many other faults in the
67 area surrounding these two main volcanotectonic structures (Fig. 1) (e.g. Dávila–Harris and Carrasco–Núñez,
68 2014; Norini et al., 2015, 2019; GEMex, 2019). In all these outcrops, the faults invariably displace the
69 Holocene Cuicuiltic Member and the underlying lava and pyroclastic units (Figs. 1 and 2; Tab. 1). These data
70 (Tab. 1) are incompatible with the U2020 conclusion that the Las Papas and Las Viboras are not faults. Indeed,
71 the data indicate that the Las Papas and Las Viboras structures have been originated in the Holocene by
72 faulting (Figs. 1 and 2, and Tab. 1) (Dávila–Harris and Carrasco–Núñez, 2014; Norini et al., 2015, 2019; GEMex,
73 2019). The U2020 description of their LH–08 outcrop can be explained by erosive retreat of the fault scarp, a
74 common process in dip–slip faults, especially in poorly consolidated sediments (e.g. Keller and Pinter, 2002;
75 Burbank and Anderson, 2011).

76

77 **2.2 Arroyo Grande and Maxtaloya faults**

78 U2020 inferred that the Arroyo Grande and Maxtaloya scarps have been generated by nowadays inactive
79 faults. U2020 stated that these faults have been active “*prior to the deposition of the Cuicuiltic Member*”. The
80 statement by U2020 arose from the analysis of two outcrops (their LH–09, see Fig. 4C, and the H6 well pad,
81 corresponding to the PDL08 outcrop of Figs. 1 and 2H), where “*strongly altered and faulted ... lavas and*
82 *ignimbrites*” are “*covered by the unaltered Cuicuiltic Member*”. Active/fossil alteration doesn’t always allow
83 identifying faults or the age of faulting, because it depends also on their depth, life span of the hydrothermal



84 system, spatial relationships, and fluid paths along primary permeability and fracture zones (e.g. Bonali et al.,
85 2016; Giordano et al., 2016).

86 Outcrops of the Arroyo Grande and Maxtaloya faults show displacements of the Cuicuiltic Member, which
87 are incompatible with the conclusion of U2020 about the age of these two structures and the correlation
88 between faulting and hydrothermal alteration (Figs. 1 and 2; Tab. 1). The field data (Figs. 1 and 2, and Tab. 1)
89 indicate that the Arroyo Grande and Maxtaloya faults have been active after the deposition of the Cuicuiltic
90 Member (Dávila–Harris and Carrasco–Núñez, 2014; Norini et al., 2015, 2019; GEMex, 2019).

91 The Maxtaloya fault trace is coincident with a sharp thermal anomaly identified by Norini et al. (2015) (Fig.
92 3). U2020 didn't consider this positive (warm) anomaly when they discussed the thermal remote sensing
93 results published by Norini et al. (2015) (Section 5.3 in U2020). The thermal remote sensing data (Fig. 3)
94 suggest that the Maxtaloya fault plays nowadays an important role in the ascent of hot geothermal fluids
95 (Norini et al., 2015, 2019; Carrasco–Núñez et al., 2017; GEMex, 2019).

96 The Maxtaloya positive thermal anomaly constitutes the southern branch of a narrow warm corridor (T1 of
97 Norini et al., 2015), which is spatially coincident with the NNW–SSE fault swarm represented by the
98 Maxtaloya fault, Los Humeros fault and some sub-parallel normal and reverse fault strands (Fig. 3) (Norini et
99 al., 2019). This 7–8 km-long thermal anomaly is incompatible with the presence of the “*shallow and
100 delocalized heat sources*” proposed by U2020 (Fig. 3). Instead, the great length of this narrow thermal
101 anomaly is consistent with a deeper pressure source driving resurgence faulting (e.g. an asymmetric cup-
102 shaped intrusion), with lower surface temperatures in the centre of the thick resurgent block (cold area to
103 the east of the 7–8 km-long warm anomaly in Fig. 3) (see Norini et al., 2015).

104

105 **3 Identification and geometry of uplifted areas: topographic data and structural mapping**

106 U2020 identified three “*main uplifted areas*” surrounding the surface expressions of the Loma Blanca, Arroyo
107 Grande and Los Humeros faults. U2020 didn't provide any information on how these uplifted areas have
108 been identified and delimited with specific and reproducible criterion. The area around the Loma Blanca fault
109 has been named by U2020 “*Loma Blanca bulge*” and described as “*a morphological bulge, 1 km in width and
110 30 m in height*”. The U2020 model also predicts the formation of an “*apical depression*” on top of a “*bulge*”
111 induced by a shallow magmatic intrusion. Indeed, U2020 depicted apical depressions on top of the three
112 “*uplifted areas*” of Loma Blanca, Arroyo Grande and Los Humeros (e.g. cross-sections in Fig. 10 by U2020).

113 Topographic profiles of the Los Potreros caldera floor extracted from a 1 m resolution Digital Elevation Model
114 (DEM) (Norini et al., 2019) show that the “*uplifted areas*” (or “*bulges*”) identified by U2020 include
115 asymmetric reliefs and depressed sectors, and have boundaries not necessarily corresponding to slope
116 changes useful for their delimitation (Figs. 1 and 4A–C). The “*Loma Blanca bulge*” defined by U2020 comprises
117 a sector of a larger and uniform westward tilted and faulted surface (Norini et al., 2019). The western
118 boundary of the “*bulge*” is in the middle of the tilted surface, while the eastern one, corresponding to a
119 normal fault, is nearly at the same elevation of the summit of the “*bulge*” (Figs. 1 and 4A) (Carrasco–Núñez
120 et al., 2017; Norini et al., 2019). Similarly, the eastern and western boundaries of the Arroyo Grande and Los
121 Humeros “*uplifted areas*” have been located by U2020 in the middle of tilted or flat surfaces. The topographic
122 data extracted from the 1 m resolution DEM (Figs. 1 and 4A–B) are incompatible with the occurrence of the
123 “*main uplifted areas*” or “*bulges*” identified by U2020. The same topographic data are also incompatible with
124 the occurrence of any “*apical depression*” along the Arroyo Grande and Los Humeros faults, suggesting that



125 the present topography of the caldera floor doesn't have any relation with the "uplifted areas", "bulges" and
126 "apical depressions" presented by U2020 (Figs. 1 and 4A-C).

127 The analogue modelling by U2020 predicts the development of reverse faults at the base of the "bulges"
128 induced by the emplacement of shallow-seated cryptodomes (e.g. Fig. 7 by U2020). U2020 didn't provide
129 any field data or other evidence (morphostructural interpretation, geophysics, well logs, etc.) locating these
130 reverse faults, which are a fundamental feature of their model. Reverse faults of this type have been
131 identified in natural cases of shallow-seated intrusions (e.g. Sibbett, 1988; Jackson and Pollard, 1990;
132 Schofield et al. 2010; Wilson et al. 2016).

133 Structural maps of the Los Potreros caldera published by Carrasco-Núñez et al. (2017); Calcagno et al. (2018);
134 Norini et al. (2019) and U2020 are inconsistent with the idea of reverse faults at the base of the "bulges"
135 identified by U2020 (Figs. 1 and 4C). The "Loma Blanca bulge" is delimited to the east by a normal fault
136 mapped by Carrasco-Núñez et al. (2017) and Norini et al. (2019) (Fig. 4A).
137

138 **4 Validation of the proposed model: geothermal wells log data**

139 One of the most significant findings of U2020 is that the uplift in the "Loma Blanca bulge" has been generated
140 by a magmatic intrusion located at 425 ± 170 m of depth. U2020 also stated that this is the heat source of
141 the local geothermal anomaly. Such a shallow depth is within the range of geothermal wells drilled in the
142 area. A validation attempt of the U2020 model in the "Loma Blanca bulge" consists in the comparison of the
143 temperature and lithological H4 well log with the predicted intrusion depth. This well is located at the top of
144 the "bulge", just to the west of its "apical depression" (Fig. 4A,C). The H4 well log should show a significant
145 temperature change and intrusive/sub-volcanic lithologies at 425 ± 170 m of depth, if a shallow-seated, still
146 hot magmatic intrusion exists beneath the "Loma Blanca bulge".

147 According to data published by Arellano et al. (2003) and U2020, the H4 stratigraphic log doesn't show any
148 evidence of intrusive bodies from the surface down to 1900 m of depth, nor a sharp increase of the
149 temperature and geothermal gradient, which remains constant (about $20^{\circ}\text{C}/100$ m) (Fig. 4D). Also, the
150 temperature profiles measured in several wells of the field (e.g. Arellano et al., 2003) don't show any strong
151 temperature inversion or sharp change in the geothermal gradient possibly correlated to recent intrusive
152 bodies at very shallow depth (" < 1 km"), nor any shallow-seated intrusive/sub-volcanic lithology (Cavazos-
153 Álvarez et al., 2020). Lithological well logs show the presence of rhyolitic-andesitic rock layers within the
154 Caldera group (mainly in the Xaltipan ignimbrite unit; Carrasco-Núñez et al., 2017), which have been
155 interpreted by U2020 as "intrusion of felsic cryptodomes within the volcanic sequence". A recent study of
156 these felsic layers, based on petrographic and geochemical analyses of borehole samples, identified them as
157 "lithic-rich breccias of local and irregular distribution that formed during the caldera collapse event" (Cavazos-
158 Álvarez et al., 2020).

159 Published well log data indicate a deeper origin of the heat source (or sources) feeding the Los Humeros
160 geothermal field, with some variation of the temperature gradient due to faults and or permeability changes
161 (Fig. 4D) (e.g. Cedillo et al., 1997; Arellano et al., 2003; Cavazos-Álvarez et al., 2020).
162

163 **5 Validation of the proposed model: stratigraphic and radiometric data**

164 One of the results presented in U2020 is that "...the recent (post-caldera collapse) uplift in the Los Potreros
165 caldera moved progressively northwards ... along the Los Humeros and Loma Blanca scarps". Based on the
166 proposed U2020 uplift model, it suggests that shallow intrusions of small magmatic bodies and,



167 consequently, the volcanic feeding system moved progressively northwards. This statement presents some
168 discrepancies with the stratigraphy, geological mapping and radiometric ages published recently (Carrasco-
169 Núñez et al., 2017, 2018; Juárez-Arriaga et al., 2018), as summarised by the following points:

170 a) An obsidian dome (Qr1 Rhyolite of Carrasco-Núñez et al., 2017) has been dated using the U/Th
171 method at 44.8 ± 1.7 ka by Carrasco-Núñez et al. (2017, 2018). Its location corresponds to the obsidian
172 dome cropping out along the Los Humeros fault described in U2020 and connected with the syn-
173 post-Cuicuiltic Member eruption (7.3–3.8 ka) (Fig. 5). In U2020 there is no description of two
174 generations of obsidian domes along Los Humeros fault, nor any explanation to invalidate the
175 previous radiometric dating. Therefore, the U2020 attribution of this obsidian dome to the 7.3–3.8
176 ka volcanic activity phase appears unjustified and, consequently, weakens their model;

177 b) The most recent volcanic activity of LHVC (post-Cuicuiltic Member) is clustered in two main ages,
178 around 3.8 and 2.8 ka, as indicated by recent radiometric and paleomagnetic data (Carrasco-Núñez
179 et al., 2017; Juárez-Arriaga et al., 2018) (Fig. 5). According to these ages and the LHVC geological map
180 (Carrasco-Núñez et al., 2017), the vents feeding the post-Cuicuiltic Member volcanic activity are
181 mainly located close to the southern and south-western sectors of the Los Humeros caldera rim.
182 These data suggest that the shallow feeding system of the post-Cuicuiltic Member activity is mainly
183 located in the southern and south-western sectors of the LHVC, some kilometres far from the
184 supposed bulged areas. Also, the ages and locations of the volcanic vents do not show any
185 progressive northward shift, but a scattered activity along the Los Humeros caldera rim.

186

187 **6 Conclusion**

188 We identified several problems in the U2020 study, showing that their model does not conform to most of
189 the published geological data about the Los Potreros caldera. The boundary conditions of a model and the
190 validation of the modelling results should always be based on the geological constraints that the natural
191 prototype imposes. In our opinion, the multiple magmatic intrusion model is imposed by U2020 to the natural
192 prototype regardless of several evidences of no fit between them. This mismatch between nature and model
193 includes the age and location of faulting, identification and delimitation of uplifted areas and apical
194 depressions, temperature and lithological wells log, and stratigraphic and radiometric data. The occurrence
195 of multiple magmatic intrusions at different depths in the Los Potreros caldera is not questioned in our
196 comment. Published data indicate that the calculations and conclusions by U2020 are unlikely to have any
197 relevance to the identification of the deformation source driving caldera resurgence and the heat source
198 feeding the geothermal field. The data and interpretations discussed in our comment have scientific and
199 economic implications. Indeed, they are important to plan the best strategies for geothermal exploration and
200 production, reducing drilling risk and potential loss of investment.

201

202

203 **Data availability:** all the data presented in this paper are available upon request.

204 **Author contributions:** Gianluca Norini and Gianluca Groppelli are equally responsible for *Conceptualization*
205 (research planning), *Investigation* (field analysis, geomorphological analysis, review of well logs and
206 stratigraphic data), *Writing - Original Draft* and *Review & Editing*, and *Visualization* (figures and maps).

207 **Competing interests:** the authors declare that they have no conflict of interest.



208 **Acknowledgments**

209 The research leading to these results has received funding from the GEMex Project, funded by the European
210 Union's Horizon 2020 research and innovation programme under grant agreement No. 727550. We thank
211 the Handling Topical Editor Joachim Gottsmann for providing valuable comments on an earlier version of the
212 manuscript. We also greatly thank Luca Ferrari and Joan Marti for the positive comments to our manuscript.
213

214 **References**

- 215 Arellano, V.M., Garcia, A., Barragan, R.M., Izquierdo, G., Aragon, A., Nieva, D., 2003. An updated conceptual
216 model of the Los Humeros geothermal reservoir (Mexico). *J. Volcanol. Geotherm. Res.* 124, 67–88.
- 217 Bonali, F., Corazzato, C., Bellotti, F., and Gropelli, G. (2015). Active tectonics and its interactions with
218 Copahue volcano. In F. Tassi, O. Vaselli, & A.T. Caselli (eds.), *Copahue Volcano*, Springer, Berlin Heidelberg,
219 23–45.
- 220 Burbank D.W. and Anderson R.S. (2011). *Tectonic Geomorphology*. Second Edition, John Wiley & Sons, Ltd,
221 Chichester, UK. 274 pp.
- 222 Calcagno, P., Evanno, G., Trumpy, E., Gutiérrez-Negrín, L. C., Macías, J. L., Carrasco-Núñez, G., and Liotta, D.,
223 2018, Preliminary 3-D geological models of Los Humeros and Acoculco geothermal fields (Mexico)–H2020
224 GEMex Project: *Advances in Geosciences*, v. 45, p. 321.
- 225 Carrasco-Núñez, G., Hernández, J., De León, L., Dávila, P., Norini, G., Bernal, J.P., Jicha, B., Navarro, M., López-
226 Quiroz, P., and Digitalis, T.: Geologic Map of Los Humeros volcanic complex and geothermal field, eastern
227 Trans-Mexican Volcanic Belt, *Terra Digitalis*, 1, 1–11,
228 <https://doi.org/10.22201/jgg.terradigitalis.2017.2.24.78>, 2017.
- 229 Carrasco-Núñez, G., Bernal, J. P., Davila, P., Jicha, B., Giordano, G., and Hernández, J.: Reappraisal of Los
230 Humeros volcanic complex by new U/Th zircon and 40Ar/39Ar dating: Implications for greater geothermal
231 potential, *Geochem. Geophys. Geosy.*, 19, 132–149, 2018.
- 232 Cavazos-Álvarez J.A., Carrasco-Núñez G., Dávila-Harris P., Peña D., Jáquez A., Arteaga D. (2020). Facies
233 variations and permeability of ignimbrites in active geothermal systems; case study of the Xáltipan ignimbrite
234 at Los Humeros Volcanic Complex. *Journal of South American Earth Sciences*, 104, 102810.
- 235 Cedillo, F., 1997. *Geología del subsuelo del campo geotermico de Los Humeros, Pue.* Internal Report
236 HU/RE/03/97, Comision Federal de Electricidad, Gerencia de Proyectos Geotermoelectricos, Residencia Los
237 Humeros, Puebla, 30 pp.
- 238 Dávila-Harris, P. and Carrasco-Núñez, G.: An unusual syn-eruptive bimodal eruption: The Holocene Cuicuiltic
239 Member at Los Humeros caldera, Mexico, *J. Volcanol. Geoth. Res.*, 271, 24–42,
240 <https://doi.org/10.1016/j.jvolgeores.2013.11.020>, 2014.
- 241 Ferriz, H., Mahood, G., 1984. Eruptive rates and compositional trends at Los Humeros volcanic center, Puebla,
242 Mexico. *J. Geophys. Res.* 89, 8511–8524.
- 243 GEMex (2019). Final report on active systems: Los Humeros and Acoculco. Deliverable 4.1. GEMex project
244 technical report, Horizon 2020, European Union, 334 pp. www.gemex-h2020.eu.



- 245 Giordano G., Ahumada F., Aldega L., Baez W., Becchio R., Bigi S., Caricchi C., Chiodi A., Corrado S., De
246 Benedetti A., Favetto A., Filipovich R., Fusari A., GropPELLI G., Invernizzi C., Maffucci R., Norini G., Pinton A.,
247 Pomposiello C., Tassi F., Taviani S., Viramonte J. (2016). Preliminary data on the structure and potential of
248 the Tocomar geothermal field (Puna plateau, Argentina). *Energy Procedia*, 97, 202–209.
- 249 Jackson M.D., Pollard D.D.: Flexure and faulting of sedimentary host rocks during growth of igneous domes,
250 Henry Mountains, Utah, *Journal of Structural Geology*, 12 (2), 185-206, 1990.
- 251 Juárez-Arriaga, E., Böhnell, H., Carrasco–Núñez, G., Nasser Mahgoub, A. (2018). Paleomagnetism of Holocene
252 lava flows from Los Humeros caldera, eastern Mexico: Discrimination of volcanic eruptions and their age
253 dating. *Journal of South American Earth Sciences*, 88, 736-748.
- 254 Keller, E.A. and Pinter, N. (2002). *Active Tectonics: Earthquakes, Uplift, and Landscape*. Second Edition.
255 Prentice Hall, Upper Saddle River, 361 pp.
- 256 Norini, G., GropPELLI, G., Sulpizio, R., Carrasco–Núñez, G., Dávila–Harris, P., Pellicoli, C., Zucca, F., and De
257 Franco, R.: Structural analysis and thermal remote sensing of the Los Humeros Volcanic Complex:
258 Implications for volcano structure and geothermal exploration, *J. Volcanol. Geoth. Res.*, 301, 221–237,
259 <https://doi.org/10.1016/j.jvolgeores.2015.05.014>, 2015.
- 260 Norini, G., Carrasco–Núñez, G., Corbo–Camargo, F., Lermo, J., Hernández Rojas, J., Castro, C., Bonini, M.,
261 Montanari, D., Corti, G., Moratti, G., Chavez, G., Ramirez, M., and Cedillo, F.: The structural architecture of
262 the Los Humeros volcanic complex and geothermal field, *J. Volcanol. Geoth. Res.*, 381, 312–329,
263 <https://doi.org/10.1016/j.jvolgeores.2019.06.010>, 2019.
- 264 Schofield, N., Stevenson, C., & Reston, T. Magma fingers and host rock fluidization in the emplacement of
265 sills. *Geology*, 38(1), 63-66, 2010.
- 266 Sibbett, B.S. Size, depth and related structures of intrusions under stratovolcanoes and associated
267 geothermal systems. *Earth-Sci. Rev.*, 25: 291-309, 1988.
- 268 Urbani, S., Giordano, G., Lucci, F., Rossetti, F., Acocella, V., and Carrasco–Núñez, G.: Estimating the depth and
269 evolution of intrusions at resurgent calderas: Los Humeros (Mexico), *Solid Earth*, 11, 527–545,
270 <https://doi.org/10.5194/se-11-527-2020>, 2020.
- 271 Wilson P.I.R., McCaffrey K.J.W., Wilson R.W., Jarvis I., Holdsworth R.E. Deformation structures associated
272 with the Trachyte Mesa intrusion, Henry Mountains, Utah: Implications for sill and laccolith emplacement
273 mechanisms, *Journal of Structural Geology*, 87, 30-46, <https://doi.org/10.1016/j.jsg.2016.04.001>, 2016.

274

275 **Figure Captions**

276 **Figure 1:** volcanotectonic map of the Los Potreros caldera area, on a DEM (illuminated from the E) (modified
277 from GEMex, 2019 and Norini et al., 2019). Las V.F.: Las Viboras fault; Arroyo G.F.: Arroyo Grande fault; Loma
278 B.F.: Loma Blanca fault. Location of outcrops in Fig. 2 and Tab. 1 is shown. Traces of A–A'–A''–A''' and B–B'
279 topographic profiles of Fig. 4 are also shown.

280 **Figure 2:** photographs of faults in the Cuicuiltic Member along the structures mapped in Fig. 1.



281 **Figure 3:** enhanced surface kinetic temperature (SKT) of the Los Potreros caldera obtained from ASTER AST08
282 night-time thermal remote sensing data (see Norini et al., 2015, for details on methods and results).
283 Examples of field-validated sources of thermal anomaly are shown in the insets (Norini et al., 2015, 2019).
284 Thermal satellite data: credits LP-DAAC, USGS EROS data center at the NASA. Satellite images in the insets:
285 credits Esri, DigitalGlobe, GeoEye.

286 **Figure 4:** topographic profiles along the **(A)** A–A'–A''–A''' and **(B)** B–B' traces shown in Fig. 1, and **(C)** schematic
287 geological map (modified from U2020) outlining the three uplifted areas discussed by U2020; the traces of
288 the two topographic profiles and the locations of the H4 and H20 well are also shown. **(D)** H4 lithological and
289 temperature log (well data from Arellano et al., 2003, and U2020). P.c.: Post-caldera group.

290 **Figure 5:** map of the post-Cuicuiltic Member vents and ages based on radiometric data, paleomagnetic
291 analysis or inferred from geological map (Carrasco-Núñez et al., 2017, 2018; Juárez-Arriaga et al., 2018). The
292 post-Cuicuiltic Member uplifted areas and obsidian dome proposed by U2020 are also shown. Active faults
293 are from Norini et al. (2019).

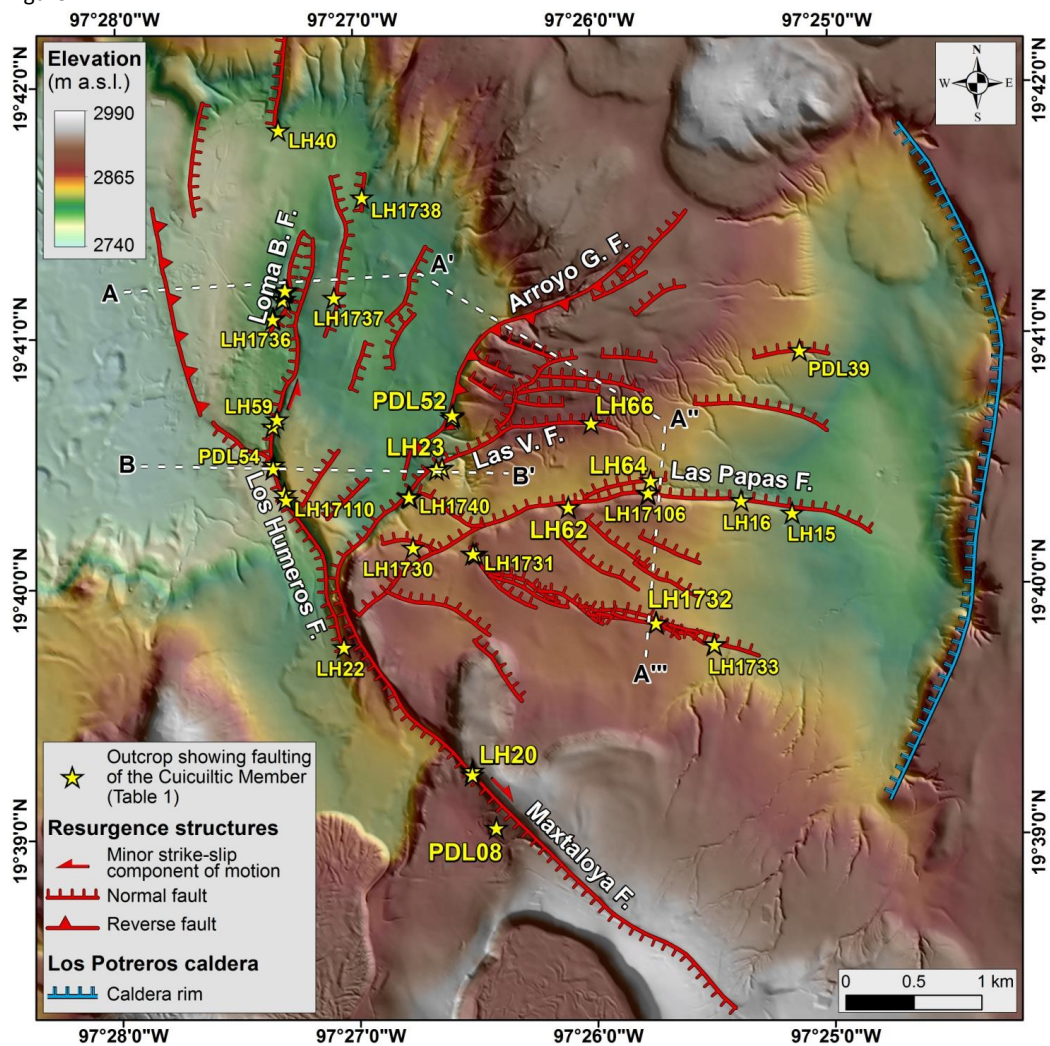
294 **Table 1** (supplementary data): field data of faults and fractures deforming the Cuicuiltic Member and the
295 underlying units (see Fig. 1 for outcrops location).

296

297



298 Figure 1:

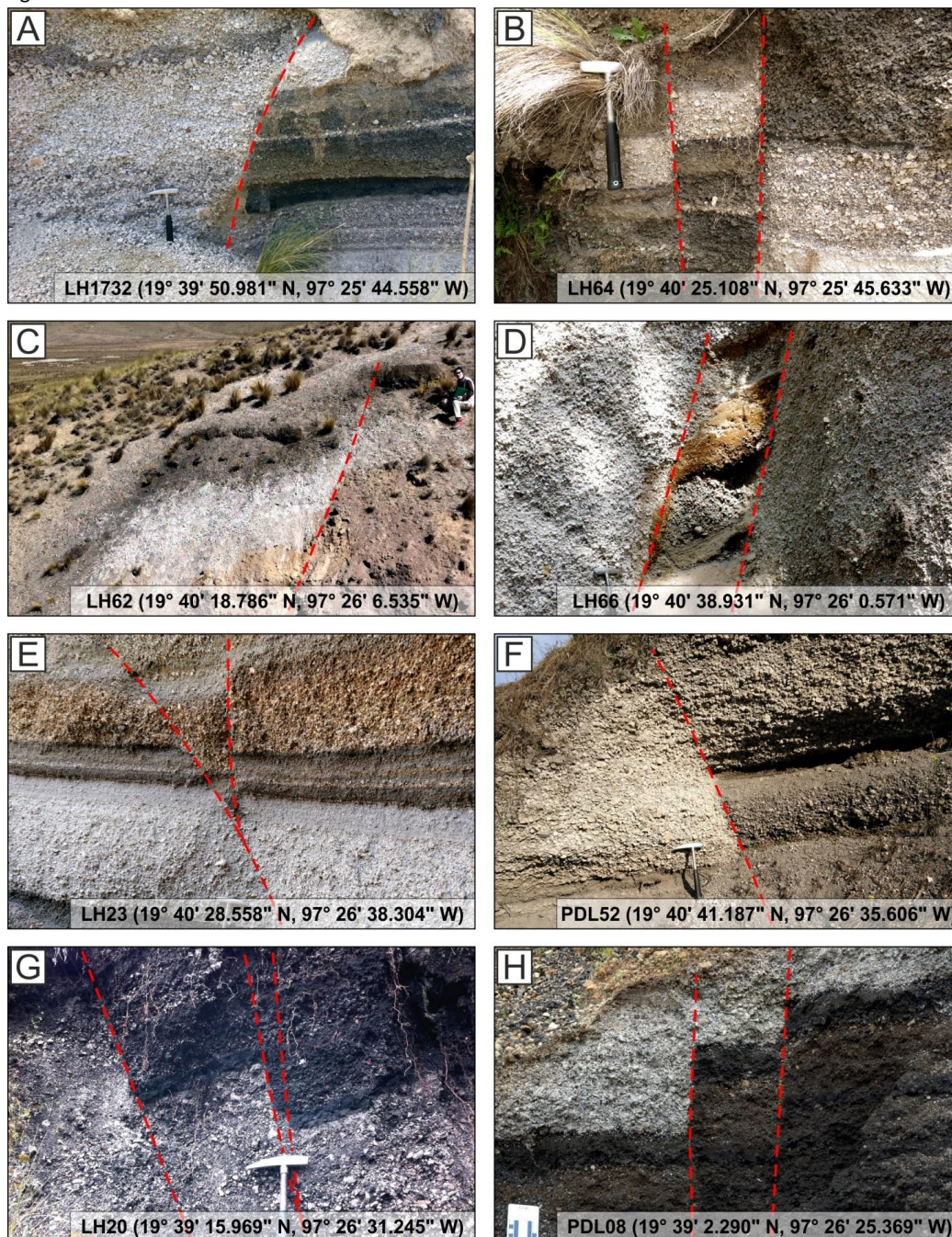


299

300



301 Figure 2:

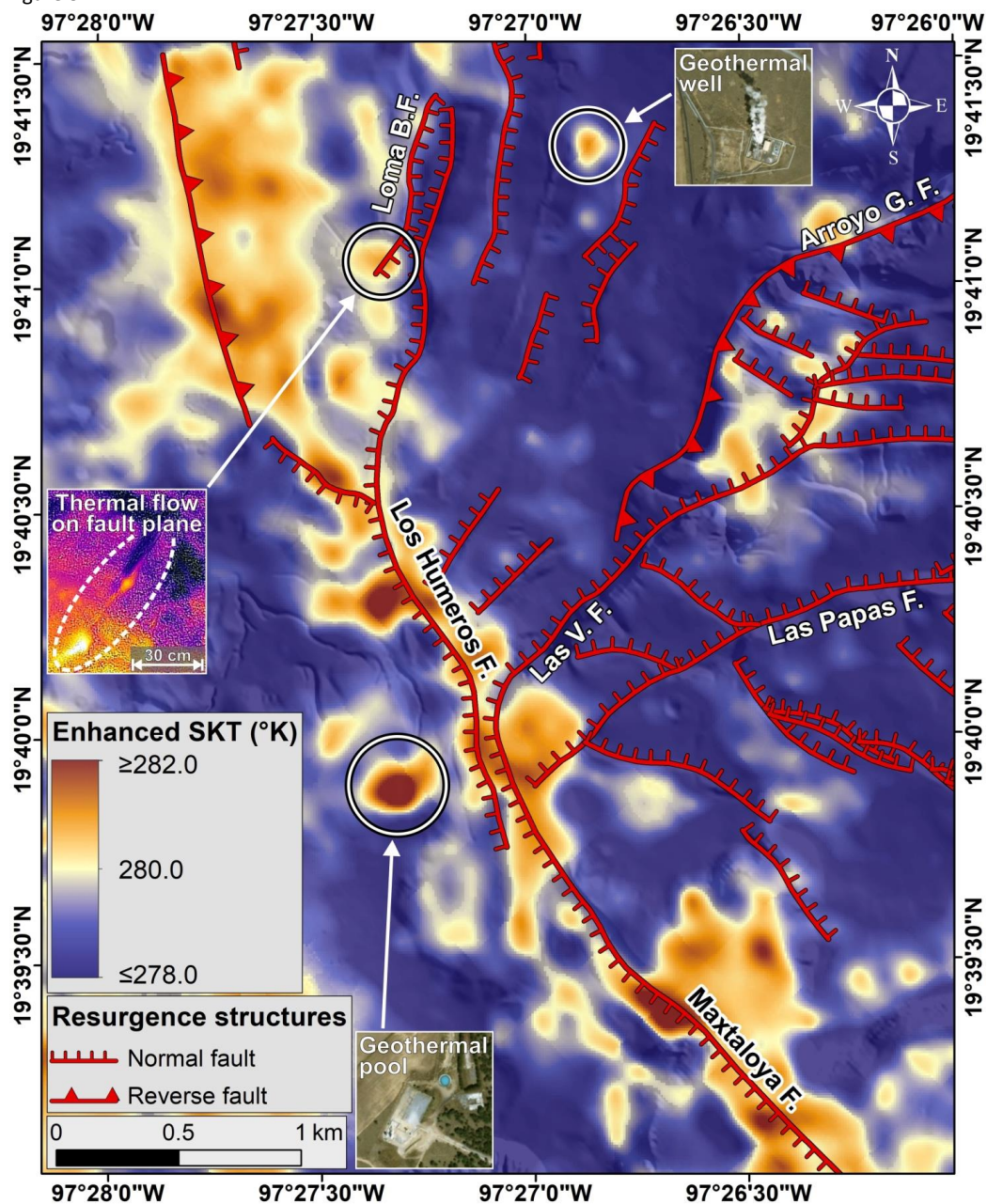


302

303



304 Figure 3:

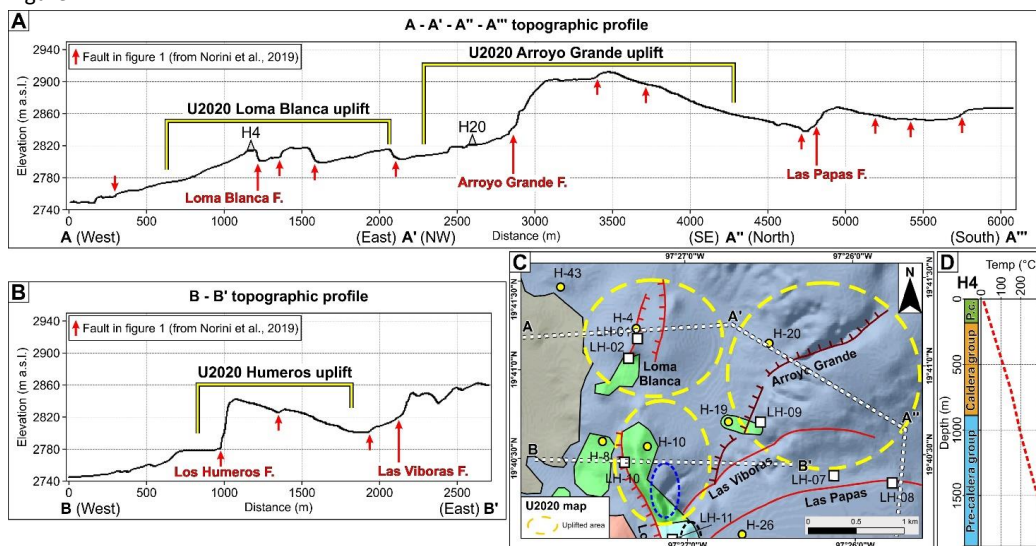


305

306



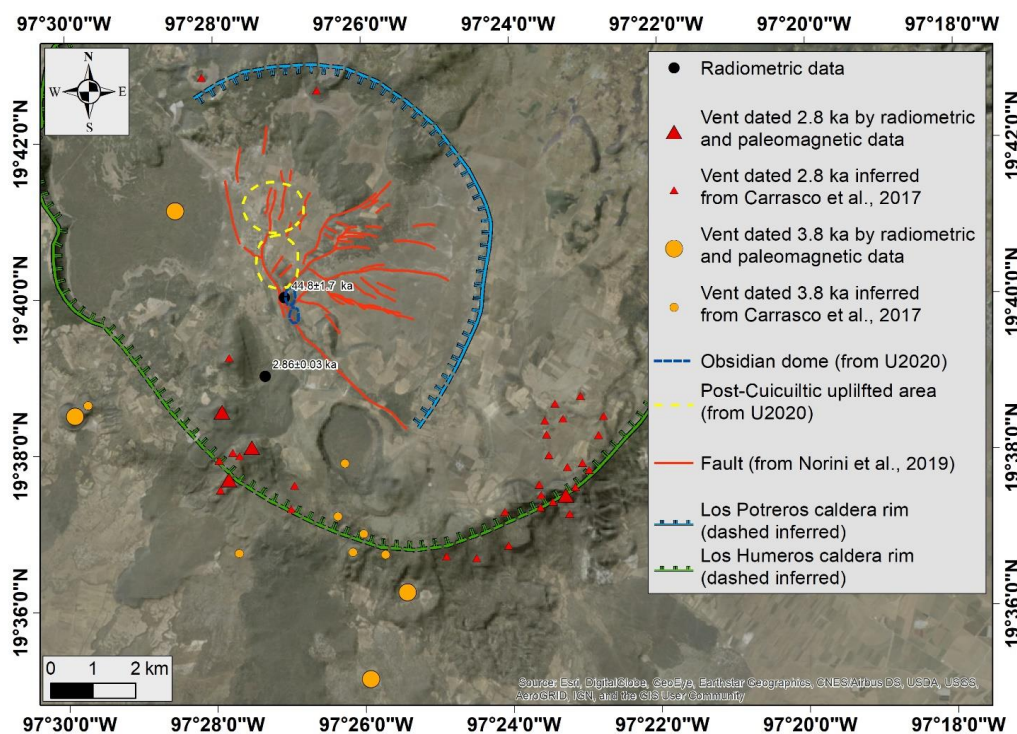
307 Figure 4:



308

309

310 Figure 5:



311

312